Developmental Biology 355 (2011) 324–333

Contents lists available at ScienceDirect

Developmental Biology

journal homepage: www.elsevier.com/developmentalbiology

FLRT3 as a key player on chick limb development

Ana Raquel Tomás [a,b], Ana Catarina Certal [a], Joaquín Rodríguez-León [a,b,*]

[a] Instituto Gulbenkian de Ciência, Rua da Quinta Grande 6, 2780-156 Oeiras, Portugal
[b] Dept. de Anatomía Humana, Biología Celular y Zoología, Facultad de Medicina, Universidad de Extremadura, Avda de Elvas s/n, 06006 Badajoz, Spain

ARTICLE INFO

Article history:
Received for publication 20 September 2010
Revised 26 April 2011
Accepted 28 April 2011
Available online 6 May 2011

Keywords:
flrt3
AER
Limb development
Chicken

ABSTRACT

Limb outgrowth is maintained by a specialized group of cells, the apical ectodermal ridge (AER), a thickening of the limb epithelium at its distal tip. It has been shown that fibroblast growth factor (FGF) activity and activation of the Erk pathway are crucial for AER function. Recently, FLRT3, a transmembrane protein able to interact with FGF receptors, has been implicated in the activation of ERK by FGFs. In this study, we show that *flrt3* expression is restricted to the AER, co-localizing its expression with *fgf8* and pERK activity. Loss-of-function studies have shown that silencing of *flrt3* affects the integrity of the AER and, subsequently, its proper function during limb bud outgrowth. Our data also indicate that *flrt3* expression is not regulated by FGF activity in the AER, whereas ectopic WNT3A is able to induce *flrt3* expression. Overall, our findings show that *flrt3* is a key player during chicken limb development, being necessary but not sufficient for proper AER formation and maintenance under the control of BMP and WNT signalling.

Introduction

During limb development, the apical ectodermal ridge (AER) is the organizing center that controls proximo-distal outgrowth. This thickening of ectodermal cells at the most distal part of the limb bud is responsible for maintaining the underlying mesenchymal cells in an undifferentiated and proliferative state. The importance and requirement of the AER are a conserved feature in the process of vertebrate limb development (reviewed in Fernandez-Teran and Ros, 2008). Although extensive studies have been carried out, the molecular mechanisms controlling the initiation and maintenance of the AER are still far from understood.

Territories in the limb bud are defined by restricted patterns of gene expression. Among these, *fgf8* is expressed in the AER; *wnt7a* is specifically expressed in the dorsal limb ectoderm and *engrailed-1* (*en-1*) in the ventral ectoderm. At the mesoderm, *Lmx-1* is expressed in its dorsal compartment and *shh* in the posterior mesenchyme (reviewed in Fernandez-Teran and Ros, 2008). The dynamic interactions between these molecules during limb bud initiation and development are very important for the correct positioning and structure of the AER.

Maintenance of limb bud outgrowth is due to the action of signals emanating from the AER, namely FGF8, that are able to induce the expression of *fgf10* in the underlying mesenchyme which, in turn, signals back to the AER resulting in the establishment of a reciprocal positive feedback loop responsible for each one's expression (Lizarraga et al., 1999; Xu et al., 1998). It has been also established that the Wnt/β-catenin activity, in particular Wnt3a, is required for the induction of *fgf8* expression in the AER (Kawakami et al., 2001; Logan, 2003).

At the intracellular level, FGF activity induces different MAP kinase cascades, including the Ras/ERK pathway in the AER and the PI3K pathway in the distal mesenchyme. As a result, during limb bud development, phosphorylated ERK1/2 (pERK) can be detected in the AER and in the mesenchyme, where FGF8 is responsible for the induction of ERK inhibitor, *mkp3*, through PI3 kinase activation. In this context, the activation of ERK in the AER is responsible for its integrity and proper function, and MKP3 antagonism in the distal mesenchyme accounts for cell survival in that area (Corson et al., 2003; Eblaghie et al., 2003; Kawakami et al., 2003; Smith et al., 2006).

Members of the Fibronectin Leucine-Rich Transmembrane (*flrt*) gene family encode putative single-pass transmembrane proteins with conserved domain structure among vertebrates, which include a putative signal peptide, ten leucine-rich repeats (LRR), a type III fibronectin domain (FNIII), a transmembrane domain, and a short intracellular tail (Haines et al., 2006; Lacy et al., 1999).

FLRT3 is the family member that has been more extensively characterized (Bottcher et al., 2004; Haines et al., 2006).

Xenopus flrt3 was identified as a gene with a similar expression pattern to FGF signalling molecules, particularly at the midbrain/hindbrain boundary (Bottcher et al., 2004). It is involved in the activation of ERK by FGFs. Moreover, it has been described that *flrt3* is able to modulate FGF signalling, to interact with the FGF receptor enhancing the activation of the FGF pathway and to be regulated by

* Corresponding author at: Departamento de Anatomía, Biología Celular y Zoología, Facultad de Medicina, Universidad de Extremadura, Avda de Elvas s/n, 06006 Badajoz, Spain. Fax: +34 924276350.
E-mail addresses: artomas@igc.gulbenkian.pt (A.R. Tomás), acertal@igc.gulbenkian.pt (A.C. Certal), jrleon@unex.es (J. Rodríguez-León).

0012-1606/$ – see front matter © 2011 Elsevier Inc. All rights reserved.
doi:10.1016/j.ydbio.2011.04.031

FGF signalling (Bottcher et al., 2004). In the mouse, *flrt3* mRNA was detected in regions known to express FGF signalling components and in areas affected by FGF signalling (Haines et al., 2006). As an example, *Flrt3* activity at the midbrain/hindbrain boundary in mouse correlates with the role of FGFs in the formation of and signalling from the isthmus (Carl and Wittbrodt, 1999; Trokovic et al., 2003). *Flrt3* knockout embryos exhibit defects in ventral closure, headfold fusion and definitive endoderm migration, as well as rupture of the anterior visceral endoderm caused by disarrangement of the basal membrane, suggesting that cell adhesion is affected upon *flrt3* ablation (Egea et al., 2008; Maretto et al., 2008).

Here we show that expression of the chicken *flrt3* in the AER co-localizes with FGF expression and ERK activation, supporting the known role of FGFs in limb formation (Lewandoski et al., 2000; Smith and Tickle, 2006). We also show that *flrt3* is an important player during chicken limb development maintaining the integrity and proper activity of the AER during limb bud development under the control of BMP and WNT signalling.

Materials and methods

Chicken embryo manipulation

Rhode Island Chicken embryos were incubated at 37.5 °C for 1.5 to 7 days. Embryos between stage 10 and 31 HH (Hamburger and Hamilton, 1951) were fixed at 4 °C in 4% paraformaldehyde (PFA) in PBS for 2 hours and overnight for immunostaining and *in situ* hybridization, respectively. Experimental manipulations of limb buds were performed always in the right wing leaving the left one as a control. Upon manipulation, eggs were sealed with tape, incubated for different periods of time and treated for further processing.

Bead implantation

Ion exchange (AG1-*X2*, Bio-Rad) or heparin acrylic beads (Sigma) were washed in DMSO and PBS with 0.1% BSA, respectively, and then incubated in the selected molecule. AG1-*X2* beads were soaked in the Fgf receptor kinase inhibitor SU5402 (Calbiochem) at a final concentration of 2 μg/μl in DMSO. The remaining proteins used in this study were soaked in heparin acrylic beads at the following concentrations: FGF2, FGF8, FGF10 and FGF19 at 1 μg/μl; BMP2, BMP4, WNT3A at 0.1 μg/μl. Beads were implanted in stage 19-21HH developing chick limb buds as described previously (Montero et al., 2001). Beads soaked in PBS with 0.1% BSA or in DMSO were implanted as a control. For each protein, between ten to fifteen embryos, divided by two rounds of *in situ* hybridizations, were analyzed for differences regarding *flrt3* expression.

Cloning of full-length and dsRNA flrt3 constructs

Full-length flrt3

Full-length *flrt3* (XM_426107) was obtained after a two-step PCR amplification of chicken RNA collected from embryos at stage 14, 21 and 25 HH using High Fidelity PCR Master kit (Roche) and subsequent cloning into an empty modified expression vector, pCAGGS-PL4 (provided by A. Raya). The following primers were used for PCR amplification: PA (FW), 5′-ATGGCAACCATCACAAAATTTACTC-3′; PB (RV), 5′-TCATGAGTGTGAATGATCTGAATCTGG-3′; P1 (FW), 5′-CCACGGATTAGGAGACAAGG-3′; P2 (RV), 5′-GCTGAGTTATGTTGTC-CAGG-3′. Successful cloning was confirmed by DNA sequencing.

dsRNA against flrt3

According to the pSUPER RNAi manufacturer system, a unique 19-nt sequence derived from the mRNA transcript of the gene targeted for suppression was designed (through iRNAi software from Mekentosj Inc.) (Brummelkamp et al., 2002), and the following oligos containing *Bgl*II and *Hind*III sites, as well as the hairpin sequence, were assembled as described by the manufacturer: forward primer, 5′-GATCCCCTTTCAGGCTACTGCTGCGATTCAAGAGATCGCAGCAGTAGCCT-GAAATTTTTGGAAA-3′; reverse primer, 5′-AGCTTTTCCAAAAATTT-CAGGCTACTGCTGCGATCTCTTGAATCGCAGCAGTAGCCTGAAAGGG-3′; 43.5% GC content; target sequence: 5′-AATTTCAGGCTACTGCTGC-GATT-3′. A mismatch RNAi (target sequence: 5′-AATTTCAGGCTA-GATCTGTGGTT-3′) was used as a control. The presence of the correct insert was confirmed by DNA sequencing.

Electroporation of limb ectoderm

Eggs were allowed to cool down to room temperature before starting the procedure. A mix of 0.1% Fast Green (Sigma®), 1 μg/μl pCAGGS-AGFP, and 5 μg/μl pCAGGS-*flrt3* or dsRNA-*flrt3* was prepared. Eggshell was swabbed with 70% ethanol and a small window opened (2 cm^2) overlying the embryo. The viteline membrane above the limb field was carefully torn off with fine tweezers and the right-dorsal surface of the lateral plate mesoderm was covered with the DNA or dsRNA mix. Electrodes were placed in position over and under the prospective limb, in a parallel position to each other and to the neural tube with the negative electrode over the embryo. Electroporation was performed with an Intracel TSS20 Ovodyne electroporator (Intracel LTD) using 3 pulses of 50 ms length (8 V each) with 60 ms interval.

Loss-of-function studies were achieved by co-electroporation of both pCAGGS-AGFP and dsRNA-*flrt3*. Gain-of-function studies were achieved by co-electroporation of both pCAGGS-AGFP and pCAGGS-*flrt3*. In both experiments, controls with single electroporation of a GFP expression vector, pCAGGS-AGFP were performed.

Cryopreservation, sectioning and immunohistochemistry

Chicken embryos were fixed as described above and cryoprotected in 10% sucrose in PBS overnight at 4 °C. Embryos were then embedded in 30% gelatine in the previous solution for 1 hour at 37 °C, oriented as desired into cryomolds and snap-frozen at −80 °C. Cryosections of 10–12 μm were placed into pre-coated slides and processed for immunostaining. Double immunohistochemistry for laminin (Sigma; 1:300) and FLRT3 (MAB, R&D Systems; 1:150) was performed using the manufacturer's recommended dilutions, and following standard protocols for immunohistochemistry in sections. DAPI nuclear staining was carried out following standard procedures at a final dilution of 1.5 μg/ml. Imaging was performed with a Leica SP5A OBS confocal microscope.

pERK wholemount immunostaining

Chicken embryos were collected in cold PBS and fixed for 2 hours at 4 °C in 4% PFA. Both PBS and fixative had been previously supplemented with a cocktail of Phosphatase Inhibitors (5 mM each NaF, Na_3VO_4, and Na_4P_2O7) in order to ensure the preservation of the phosphorylated form of ERK. Embryos were then passed to TBS, dehydrated to methanol and stored at −20 °C.

A 30-minute blockage of endogenous peroxidase in 6% H_2O_2 in methanol was performed prior to rehydration to TBS. The tissue was permeabilized for 30 minutes in 0.3% Triton X-100 in TBS and blocked in 0.1% Triton X-100, 3% Donkey Serum in TBS (TTBSB) for an additional 30 minutes.

Samples were then incubated with Anti-phospho-p44/42 MAPK (ERK 1/2) antibody (Rabbit monoclonal #4370; Cell Signaling) at 1:50 in the previous solution during 2 overnights at 4 °C; washed at least 4 times for 15 minutes each in 0.1% TTBSB; incubated ON at 4 °C with a Donkey anti-Rabbit-HRP conjugated antibody (Jackson ImmunoResearch Laboratories, Inc.) at 1:100 in the previous solution, and washed thoroughly in 0.1% TTBSB and finally in TBS.

Embryos were developed using the TSA™ PLUS Fluorescein System (PerkinElmer), according to the manufacturer's recommended protocol. Embryos were thoroughly washed in TBS, and observed under a fluorescent microscope.

In situ hybridization and cartilage staining

Probes for *flrt3*, *fgf8*, *en*-1, *msx1* and *lmx-1* were obtained from chicken ESTs ChEST840j5, ChEST320b9, ChEST92p12, ChEST660e20 and ChEST100c17, respectively, from Geneservice (Boardman et al., 2002). *Mkp3* and *gremlin* were obtained as previously described (Kawakami et al., 2003; Merino et al., 1999).

In situ and double *in situ* hybridization were performed as described (Furthauer et al., 2002; Pott and Fuss, 1995; Wilkinson, 1992). Alkaline phosphatase reactions were developed using BM Purple (Roche) and INT/BCIP (Roche) substrates. Specific labelling was controlled using sense RNA probes. Chicken embryos were also examined by Alcian green cartilage staining as described (Ganan et al., 1996).

Scanning electron microscopy

Chicken embryos were fixed in 2.5% glutaraldehyde/cacodylate buffer (0.1 M, pH 7.4) for 4 hours at 4 °C, washed three times in cacodylate buffer, and subsequently processed for critical point and sputtering following standard procedures. Sputtering of chicken limb buds was performed for 3 minutes. Imaging was performed in a JEOL JSM 6390LV scanning microscope.

Results

Flrt3 expression is restricted to the AER and co-localizes with fgf8 expression and pERK activity

In order to determine the role of *flrt3* in the development and patterning of the vertebrate limb, we started by examining the spatial and temporal expression pattern of *flrt3* mRNA by *in situ* hybridization and protein localization by immunohistochemistry during chicken limb development.

Chicken *flrt3* is expressed at stage 11HH in the neural ectoderm, at the developing optic placodes and in the neural crest cells around the otic placodes (Fig. 1A, white arrow). *Flrt3* transcripts are also found along the anterior–posterior (AP) axis in the somites (Fig. 1A, black arrow) and at lower levels in the presomitic mesoderm. As the somites differentiate, *flrt3* expression becomes restricted to the region of the dermomyotome closer to the neural tube (Fig. 1B, arrows). *Flrt3* can also be found in the head at the midbrain–hindbrain boundary, in the optic vesicle (Fig. 1B, D black arrow), in the branchial arches (Fig. 1B, C, D white arrow) and in the tail bud.

During limb bud development, *flrt3* transcripts are first detected in the ectoderm of the prospective limb fields at stage 14HH (Supplemental Fig. 1A). By stage 16–18HH expression expands over the whole ectoderm of the limb bud (Fig. 1B, E) and as the limb bud grows and the limb ectoderm condenses to form the Apical Ectodermal Ridge, *flrt3* expression becomes restricted to the thickened ectoderm of the AER (Fig. 1C–D), co-localizing with *fgf8* and pERK activity (Fig. 3E′) (Kawakami et al., 2003; Mahmood et al., 1995). *Flrt3* expression at the AER is maintained during limb bud outgrowth, disappearing as the AER regresses (Fig. 1E–H).

The presence of specific AER *flrt3* mRNA transcripts can be observed in a transverse section of a stage 22HH forelimb (Fig. 1I).

There is a clear delay in expression along the AP axis. Although *flrt3* expression pattern is identical in both forelimbs and hindlimbs, *flrt3* expression in hindlimbs is delayed.

Immunohistochemistry studies were performed in sections of stage 14HH to 29HH chick embryos. We have identified FLRT3 protein in cells that constitute the developing limb, dermomyotome, branchial arches, and the developing retina, correlating with the structures where the *flrt3* mRNA was expressed.

During limb bud development FLRT3 is immunolocalized at stage 14–15HH all over the ectoderm and as the ectoderm condenses to

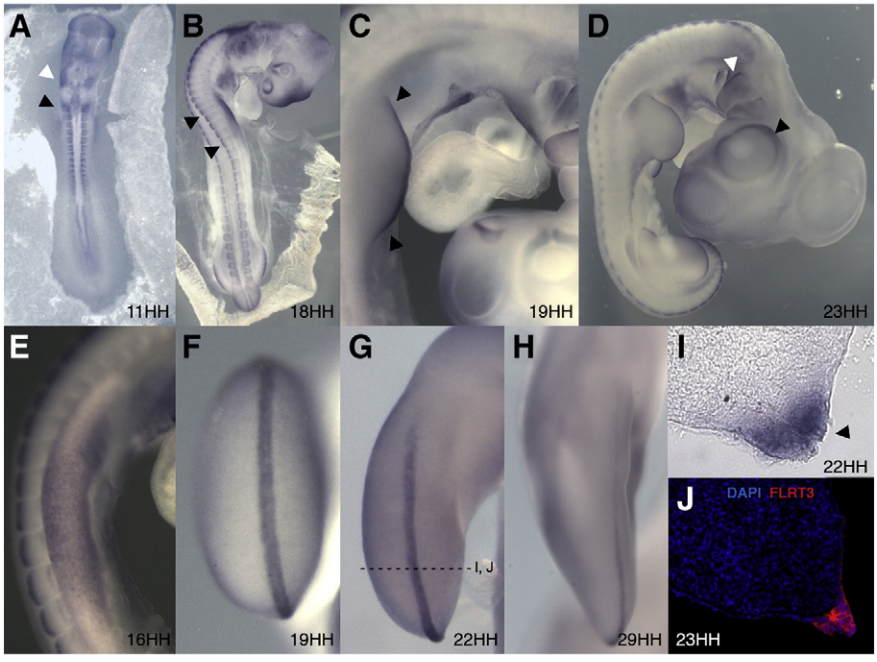

Fig. 1. Expression pattern of *flrt3* in *Gallus gallus.* A, Chicken embryo at stage 11HH; arrows indicate localized expression of *flrt3* in the somites (black arrow) and around the otic placodes (white arrow). B, Chicken embryo at stage 18HH, *flrt3* expression is restricted to the epaxial dermomyotome closer to the neural tube (arrows). At 19 and 23HH (C and D) *flrt3* is expressed in the apical ectodermal ridge (AER, arrows in C), the developing eye (D, black arrow) and in the branchial arches (D, white arrow). E–H, A series of stages can be observed where condensation of epithelial cells that will form the AER becomes evident due to *flrt3* staining, beyond stage 19HH to stage 29HH *flrt3* expression is restricted to AER. I, Transverse section of a stage 22HH limb bud. J, Immunohistochemistry in a stage 23HH cross section, showing specific membrane staining of AER cells with anti-FLRT3 antibody (red), nuclei are counterstained with DAPI (blue).

Table 1
Phenotypes upon functional studies. pCAGGS-AGFP and mismatch *Flrt3* RNAi electroporation used as controls.

	Phenotype observed	No. of limbs	Percentage limbs	
AGFP	Normal	81		93%
	Abnormal	6		7%
	Total	87		
Mismatch	Normal	54		92%
Flrt3 RNAi	Abnormal	5		8%
	Total	59		
Flrt3 RNAi	Normal	86		69%
	Slightly square	10	8%	
	Indented	20	16%	31%
	Mild truncation	6	5%	
	Truncation	2	2%	
	Total	124		
Full-length	Normal	53		38%
Flrt3	Enlargements	37	27%	
	Projections	10	7%	62%
	Both	38	28%	
	Total	138		

form the AER, the FLRT3 protein becomes restricted to the distal ectodermal cells (stage 18HH; Supplemental Fig. 1B). Finally, it localizes to the AER and a small portion of the surrounding ectoderm (Fig. 1J) until it completely disappears with the regression of the structure.

Overexpression of flrt3 induces pERK and fgf8 positive ectopic ridges and enlargements of the pre-existing AER

In gain- and loss-of-function experiments in *Xenopus*, FLRT3 was shown to mediate FGF signalling (Bottcher et al., 2004). Considering the key importance of FGF in limb initiation and outgrowth, we investigated the role of *flrt3* in the formation and maintenance of the AER.

A pCAGGS-*flrt3* vector was co-electroporated with pCAGGS-AGFP (control) into the ectoderm of stage 13–14HH chicken limb fields, and expression was examined 24 hours to 96 hours post-electroporation. Electroporation with pCAGGS-AGFP alone induced no significant changes in gene expression or limb morphology. Phenotypes obtained with overexpression of *flrt3* on limb ectoderm could be mainly classified in two groups (Fig. 3D, C′): enlargements and projections of the AER. Such phenotypes were observed in 62% of pCAGGS-*flrt3* electroporated embryos ($n = 138$) (Table 1).

Limb outgrowth is maintained by a constant crosstalk between different tissues, thus becoming relevant to analyze the effect of a shift in this fine-tuned molecular balance. Excess of *flrt3* transcripts gives rise to enlargements of the pre-existing AER both over the

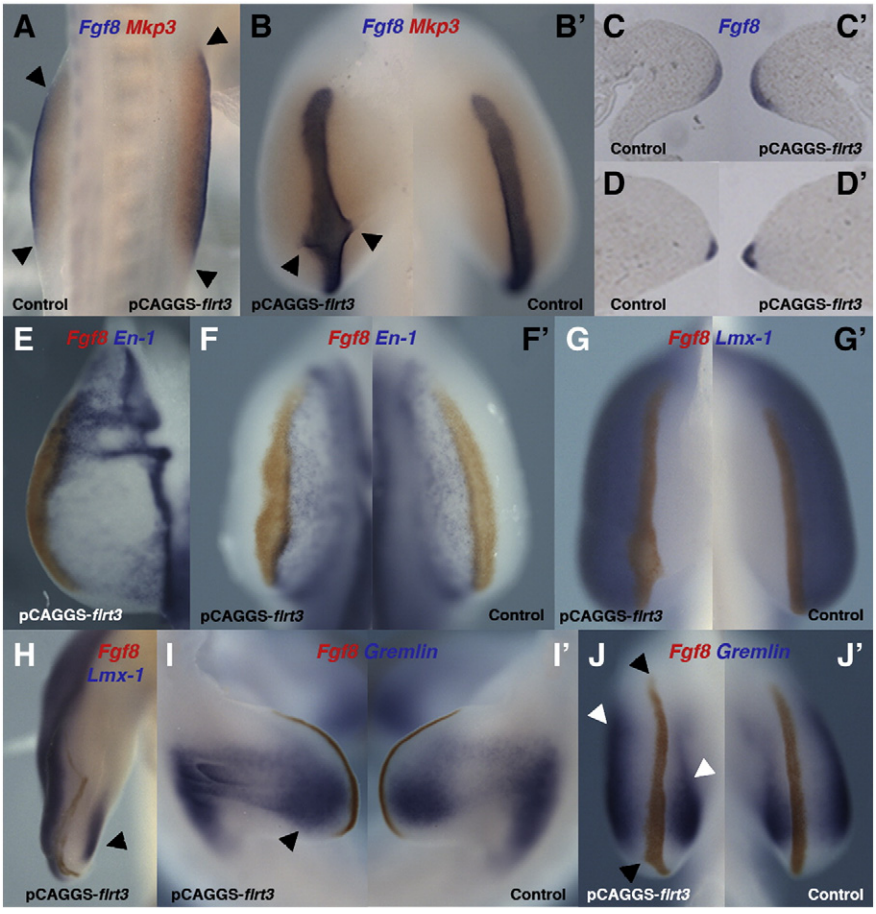

Fig. 2. Gain-of-function studies for *flrt3* in *Gallus gallus*. Embryos electroporated with an expression pCAGGS vector harbouring the full-length chicken *flrt3* cDNA: 24 hours, 48 hours and 72 hours after manipulation. A, B, C′, D′, E, F, G, and H–K are manipulated limbs. B′, C, D, F′, G′ are counterlateral control limbs. A–B′, Double *in situ* hybridization for *fgf8* (blue) and *mkp3* (red) expression 24 hours (A) and 48 hours (B, B′) post-electroporation; note the extended pCAGGS-*flrt3* electroporated limb (A, arrows) compared with the control, and the AER enlargement and formation of projections in B. C–D′, Cross sections of whole mount *in situ* hybridization for *fgf8* expression (blue) showing an enlarged *fgf8*-positive AER, 24 hours (C, C′) and 48 hours (D, D′) after manipulation. E–F′, Double *in situ* hybridization for *fgf8* (red) and *en-1* (blue) expression 48 hours post-electroporation; patches of *en-1* expression are observed in the newly formed boundary upon transformation of the ectoderm with excess *flrt3*. G–I, Double *in situ* hybridization for *fgf8* (red) and *gremlin* (blue) expression 48 hours (G) and 72 hours (H) post-electroporation; the dorsal mesenchymal marker *lmx-1* extends its domain of expression towards the areas affected by excess FGF signalling (E), generating a invasion of the dorsal territory towards the ventral part (H). I–J′, Dorsal (I, I′) and top (J–J′) view of a 48 hours post-electroporation embryo stained for *fgf8* (red) and *gremlin* (blue); note the enlarged *fgf8*-stained AER (J, black arrows) and the extended *gremlin* domain in I and J.

dorso-ventral and anterior–posterior axes of the structure, which is evident from *in situ* hybridization for the AER marker *fgf8* at 24 hours and 48 hours post-electroporation (Fig. 2A, C, C′ and B, D, D′, respectively). In agreement with the increase in FGF signalling from the AER, in the mesechyme *Mkp3* shows an expansion of its expression domain (Fig. 2A, B).

At the non-AER ectoderm, excess of *flrt3* transcripts promotes the development of projections from the AER (Fig. 3A, C′). These ectopic ridges appear to be extensions of the pre-existing AER towards the dorsal and ventral sides of the limb bud: main ectopic ridges, closer to the pre-existing AER and approximately the same width (Fig. 2B, Supplemental Fig. 3A), and secondary ectopic ridges, thinner and further apart from the AER (Fig. 3C and Supplemental Fig. 3B, arrows).

Although *flrt3*-positive (Fig. 3B, Supplemental Fig. 3B), these ridges do not express *fgf8* in its full ectopic-extension (Figs. 2B, 3B, Supplemental Fig. 3A, B′). Notwithstanding, ectopic pERK in *flrt3*-electroporated limbs is detected by whole mount immunostaining, (Fig. 3E–F) not only in the pre-existing AER and its expansions, but also in the ectopic ridges after FLRT3 overexpression.

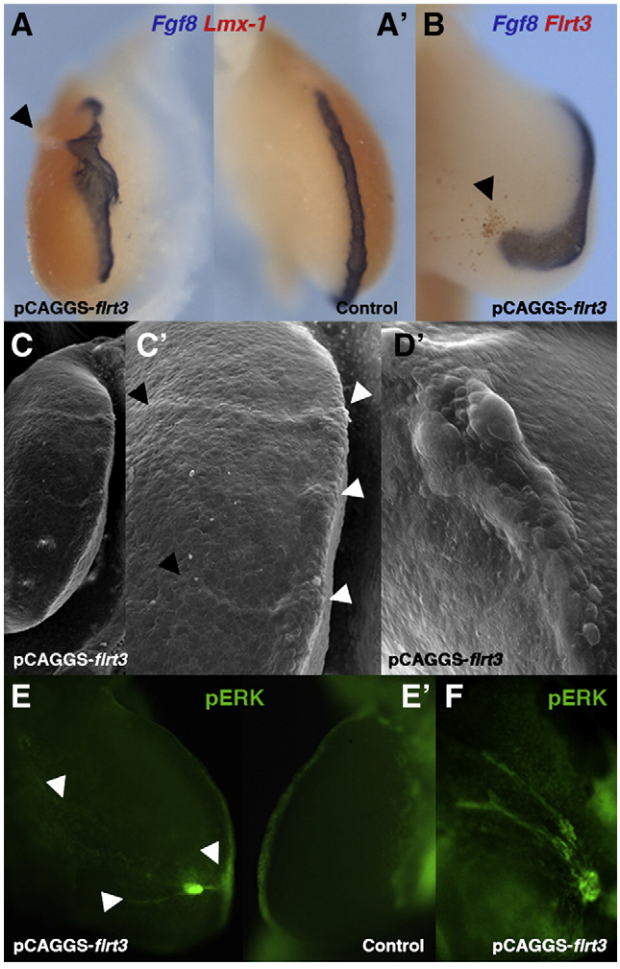

Fig. 3. Ectopic ridges are formed upon transformation of the ectoderm with excess *flrt3*. Embryos electroporated with an expression pCAGGS vector harbouring the full-length chicken *flrt3* cDNA 48 hours after manipulation. A–A′, double *in situ* hybridization for *fgf8* (blue) and *lmx-1* (red) expression; ectopic AERs induced after *flrt3* overexpression are *fgf8*-positive only in the vicinity of the original AER (A, arrow) maintaining their ectodermal identity. B, double *in situ* hybridization for *fgf8* (blue) and *flrt3* (red) expression enhancing that the presence of *fgf8*-positive cells on the *flrt3*-induced AER-like ridges only occur in close proximity of the original AER. C-D, Scanning Electron Micrograph of pCAGGS-*flrt3* electroporated embryos 72 hours after manipulation; C′ is a detail of the phenotype shown in C, zooming on the projections towards the dorsal side of the limb bud and enlargement of the pre-existing AER (D). E–F, Whole mount immunostaining against the phosphorylated form of ERK (pERK), highlighting the presence of pERK in the enlarged AER (E, arrows) and the ectopic AER-like ridges formed upon *flrt3* overexpression (F). F, Close up of pERK-positive ectopic ridges in a dorsal view of an *flrt3*-electroporated limb.

To test if AER expansions induce changes in the dorso-ventral patterning, several *in situ* hybridizations with dorso-ventral markers were performed. In the ventral ectoderm, *en*-1 expression is required to inhibit *lmx-1* expression from the dorsal mesoderm (Johnson and Tabin, 1997). Upon transformation of the ectoderm by excess *flrt3* we observe a deregulation of *en-1* expression (Fig. 2E, F). The genetic interactions involved in AER formation and specification of dorsal pattern are scrambled and the ventral ectodermal boundary is loose on the enlarged AER. The ventral *en-1*-positive ectoderm domain is absent from the enlarged ridge and patches of *en-1* expression are observed in the newly formed boundary (Fig. 2E–F′). In one case, due to the deregulation of *en-1*, the dorsal mesenchymal marker *lmx-1* extends its expression domain towards the areas affected by excess FGF signalling, generating an invasion of the dorsal territory towards the ventral part (Fig. 2H).

In order to prove that the excess of FGF signalling and subsequent enlargement of AER territory could be due to a deregulation of the FGF/BMP expression at the AER, we checked if *gremlin*, an extracellular BMP antagonist, and the main BMP antagonist required for early limb outgrowth and patterning (Khokha et al., 2003; Merino et al., 1999), was upregulated upon *flrt3* overexpression. We have observed an enlargement of *gremlin*'s expression territory towards the posterior part of the limb bud (Fig. 2I), associated with an enlargement of the AER and *fgf8* upregulation in that area (Fig. 2J).

Silencing of flrt3 affects the integrity of the AER

Given that ectopic expression of *flrt3* in the limb field of 14HH chicken embryos triggers the onset of signalling cascades that culminate in the induction of ectopic ridges, we tested if removal of the endogenous *flrt3* expression during limb bud development affects normal development.

Silencing of *flrt3* was achieved by co-electroporation into the ectoderm of both pCAGGS-AGFP (control) and a pSUPER plasmid that directs intracellular synthesis of short interfering RNA (siRNA)-like transcripts specifically targeting *flrt3*. Embryos were manipulated at stage 12–16HH, and examined 24 hours to 96 hours post-electroporation. As before, electroporation of pCAGGS-AGFP alone induced no significant changes in gene expression or limb morphology, and neither did mismatch siRNA (Table 1).

Upon *flrt3* silencing by electroporation of siRNA, 31% of the embryos presented alterations to normal limb morphology ($n=86$). A wide range of phenotypes was observed, and the severity correlates with the size of *flrt3*-siRNA + PCAGGS-AGFP electroporated area. Phenotypes obtained from silencing of *flrt3* vary from small indentations along the AER, shown by discontinued *fgf8* expression (Fig. 4A), to complete disruptions of AER integrity leading to impairment of limb development (Fig. 4G) (Table 1). Residual levels of *flrt3* expression (Fig. 4B, C) appear to be enough to promote initiation and outgrowth of the remaining limb bud (Fig. 4F).

The effect of *flrt3* silencing can also be observed in the distal mesenchyme that responds to AER signals through the loss of expression of *msx1* in distal mesenchymal cells (Fig. 4D).

Morphological effects of *flrt3* loss-of-function experiments become evident in scanning electron micrographs of a stage 27HH embryo, where the well-defined ridge normally present at the distal margin was discontinuous or completely absent in some places (Fig. 4F). In two cases, a complete lack of the limb was observed with the consequent loss of its skeletal pieces (Fig. 4G).

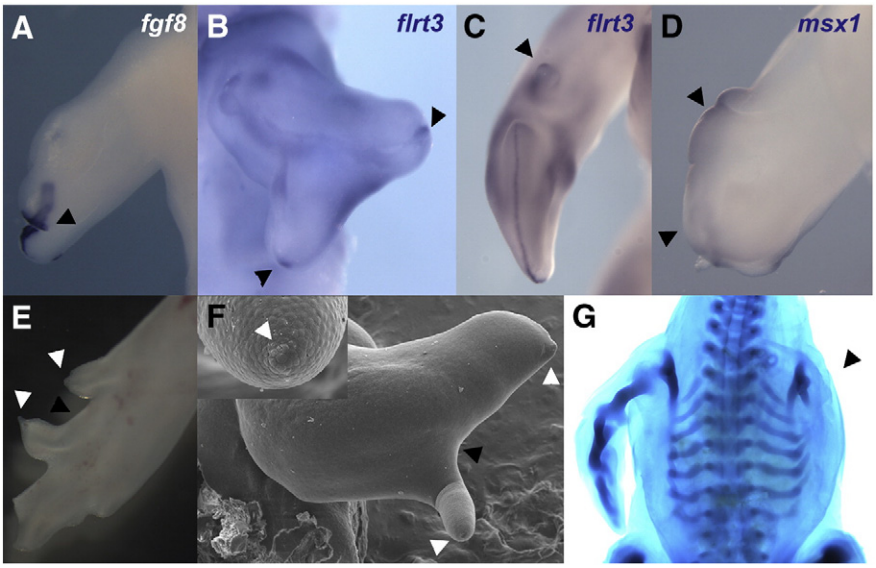

Fig. 4. Loss-of-function studies for *flrt3* in *Gallus gallus*. A–C, AER loss of integrity in embryos 72 hours post-*flrt3*-dsRNA electroporation as shown by *in situ* hybridization for *fgf8* (A) and *flrt3* (B, C). D, *In situ* hybridization for the distal mesenchyme marker *msx1*, also affected by *flrt3* downregulation. E, Observed phenotype 96 hours post-electroporation with *flrt3*-dsRNA. F, Scanning Electron Micrograph of a *flrt3*-dsRNA electroporated limb; note that a small cluster of isolated AER cells is still able to promote outgrowth of part of the limb (E, F, white arrows; close up in F). I, Complete truncation of the limb in a 72-hour*flrt3*-dsRNA electroporated embryo stained for cartilage with Alcian green.

Flrt3 expression is not regulated by FGF activity, although ectopic Wnt3a is able to induce flrt3

Studies by Bottcher et al. (2004) suggest that expression of *xflrt3*, the *Xenopus laevis* homologue, is induced by FGF signalling. Spatial and temporal localizations of *cflrt3* during normal limb bud development as shown before (Fig. 1) together with results from gain- and loss-of-function studies suggest a key role for *flrt3* in the initiation and maintenance of the AER in *Gallus gallus*.

Therefore, we examined the involvement of key proteins during limb development in the regulation of *flrt3* expression. Beads soaked in several molecules known to be directly related to processes leading to induction, growth and shaping of the limb were applied at the most anterior part of stage 20–21HH limb buds, close to the AER. Control beads soaked in PBS showed no effect on *flrt3* expression.

Several FGF family genes are responsible for AER activity. Out of the 22 known FGF genes, six are known to be expressed in the AER (*Fgf2*, *Fgf4*, *Fgf8*, *Fgf9*, *Fgf17* and *Fgf19*). From these, *Fgf4*, *Fgf8*, *Fgf9* and *Fgf17* have been shown to be directly responsible for AER activity. Their role is to provide AER function, either directly or indirectly, controlling proximal–distal outgrowth of the bud by maintaining the distal mesenchymal cells in a proliferative state (Boulet et al., 2004; Kurose et al., 2004; Mahmood et al., 1995; Mariani et al., 2008; Martin, 1998; Niswander and Martin, 1992; Savage and Fallon, 1995).

We tested if FGF activity from the AER was able to induce *flrt3* expression. In our model, we have observed that *flrt3* expression is not induced by FGF8 beads applied to the anterior part of the AER (12 embryos; $n=15$) but instead is inhibited in a small number of samples (3/15 embryos; Fig. 5A).

SU5402 is a commercially available molecule that competes with FGFs for their receptors, therefore inhibiting its activity. SU5402 applied to the anterior distal part of the mesenchyme in close contact to the AER was shown to be responsible for the loss of expression of transcription factors such as *sp8*, 10 hours post-bead implantation (Kawakami et al., 2004). No induction or enlargement of *flrt3* expression was observed in the distal epithelium in all the limbs treated ($n=13$, Supplemental Fig. 2A).

In order to show if FGF activity from the mesenchymal cells underneath the AER is directly responsible for *flrt3* induction in the AER, we applied FGF10 beads to the developing limb. Embryos were fixed 5 hours and 10 hours post-implantation to ensure a time window where there is no induction of other signalling molecules on the AER such as *wnt3a* and *fgf8*, but where transcription factors like *sp8* are already induced (Kawakami et al., 2004). We found no alteration on *flrt3* expression in all the manipulated limbs as compared to the control ones on the same embryo ($n=12$ Fig. 5B, B′).

Because *wnt3a* is a known inducer of *fgf8* expression and because the establishment of the ridge (Barrow et al., 2003) and FGF activity do not seem to be involved on *flrt3* induction, we further looked if *wnt3a* was directly inducing *flrt3*. Limbs treated with WNT3A show an elongation of the *flrt3* expression domain in the apical ectoderm (Fig. 5C; compare arrows). Moreover, WNT3A is able to induce ectopically the expression of *flrt3* in the mesenchyme around the bead ($n=14$; Fig. 5D).

BMPs specifically inhibit flrt3 in the AER

Bone Morphogenic Proteins (BMPs), as well as FGFs and WNTs, are key signalling molecules involved in limb development. Several BMP-family members such as *bmp2*, *bmp4* and *bmp7* are expressed in the AER (Geetha-Loganathan et al., 2006), being their main roles the establishment of the dorso-ventral axis, induction of apoptosis and maintenance of the integrity of the ridge.

To study the BMP role in the control of *flrt3*, avoiding the initiation of activation of apoptotic genes by cells, embryos were sacrificed within 6 hours post-bead implantation. As a control, we performed in the same experimental limb *in situ* hybridization for *mkp3* and for *flrt3*. Results show no alteration on *mkp3* expression 3 hours and 5 hours upon bead implantation (Supplemental Fig. 2B), however a closer look at the AER shows a gap on *flrt3* expression on the area of influence of BMPs both 3 hours and 5 hours post-implantation ($n=10$; Fig. 5E).

These results support a role for BMP activity in *flrt3* inhibition.

Discussion

The coordinated and intricate network of signalling pathways is a consequence of the interaction between the organizing centers that constitute the developing vertebrate limb and is responsible for the

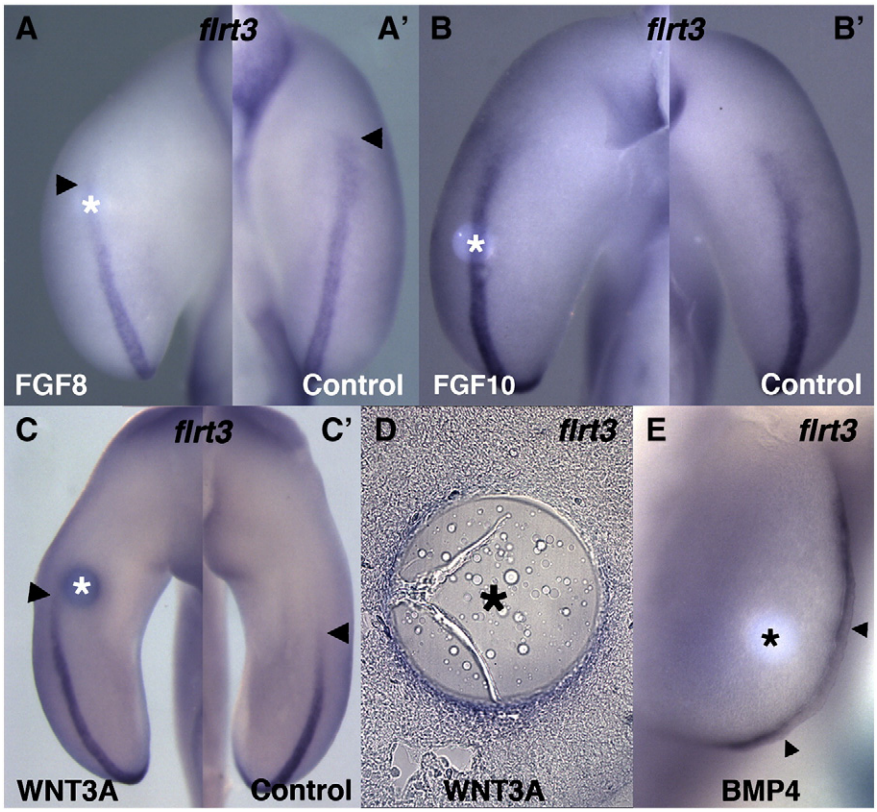

Fig. 5. Regulation studies of *flrt3* expression in *Gallus gallus* limb development. *In situ* hybridization for *flrt3*. A′, B′ and C′ are control limbs of A, B and C, respectively. A, Inhibition of *flrt3* expression 10 hours after treatment with FGF8 beads (compare arrows). B, Unaltered expression of *flrt3*, 10 hours after treatment with FGF10. C, Induction (compare arrows) of ectopic expression of *flrt3* by WNT3A, 20 hours after treatment. D, Cross section of C, showing *flrt3* ectopic expression around the WNT3A bead. E, Inhibition of *flrt3* expression 5 hours after treatment with BMP4 beads. *Bead location.

outgrowth and patterning of the limb in its three axis: anterior–posterior (AP), proximo-distal (PD) and dorso-ventral (DV).

These interactions are mediated by several families of signalling molecules such as WNTs, BMPs and FGFs and the integration of this information results in the final and proper positioning of the tissues that will form the limb (Capdevila and Izpisua Belmonte, 2001).

FGFs are very important molecules during embryonic development, being involved in numerous cell processes such as cell proliferation, differentiation, cell survival and motility (Capdevila and Izpisua Belmonte, 2001; Tickle, 2002a). FGF8 signals from the AER to the underlying mesenchyme promoting the survival of the mesoderm while sensitizing the mesodermal tissue for the pro-apoptotic effects of BMPs (Montero et al., 2001). The intracellular response to FGF8 stimuli is mediated by FGF receptors (FGFRs), which trigger several signalling pathways, namely the Ras-MAPK/ERK and the PI3K pathways.

Due to the wide range of FGFs' biological roles, and due to the variety and complexity of signalling pathways activated, FGF signalling must be tightly regulated (Sun et al., 2002; Thisse and Thisse, 2005; Xu et al., 1998). A growing number of proteins have been identified as specific regulators of FGFR-mediated FGF signalling. These molecules affect the FGF signalling cascade at different levels. Most belong to the FGF synexpression group, a set of genes that share complex spatio-temporal expression patterns and have a functional relationship. *Sprouty*, *spred*, *sef*, *shisa* and *mkp3* are known negative modulators of FGF signalling, whereas *erm*, *er81* and *pea3* promote FGF signalling (Dikic and Giordano, 2003; Furthauer et al., 2002; Furushima et al., 2007; Kawakami et al., 2003; Raible and Brand, 2001; Sivak et al., 2005; Tsang and Dawid, 2004; Zhang et al., 2001).

Flrt3 has been described in *X. laevis* as a FGF signalling positive modulator, activating the MEK/ERK signalling cascade, as opposed to MKP3, an inhibitor of the cascade through specific ERK1/2 dephosphorylation (Bottcher et al., 2004).

The co-localization of activated forms of ERK1/2 (pERK) with FGF-expressing regions during early embryonic development has been widely described (Corson et al., 2003; Eblaghie et al., 2003; Kawakami et al., 2003; Lunn et al., 2007; Smith et al., 2006). Our results support not only that *flrt3* is expressed in areas with FGF activity, as previously reported in *X. laevis* (Bottcher et al., 2004), but also that it is confined to places where ERK is phosphorylated (Figs. 1G, 3E′), such as the AER (Kawakami et al., 2003). In fact, when we overexpress *flrt3* in the limb ectoderm we observe the presence of pERK at the enlargments of the pre-existent AER and in the ectopic ridges, a direct result of the ectoderm's FGF signalling enhancement. As a consequence, there is an increase of *mkp3* expression in the mesenchyme. A similar phenotype was obtained when FGF-soaked beads were applied in the limb bud (Eblaghie et al., 2003; Kawakami et al., 2003). In the limb mesenchyme, pERK and its inhibitor, *mkp3*, are detected, but we found no expression of *flrt3* at this level, suggesting that other mechanism should be controlling ERK phosphorylation in this area.

In chicken, ectopic expression of *mkp3* results in the disruption of limb outgrowth, a phenotype characteristic of FGF signalling blockage (Bottcher et al., 2004; Eblaghie et al., 2003; Kawakami et al., 2003). When a constitutively active form of *mkp3* is overexpressed, cells at the AER are unable to translocate active ERK to the nucleus, resulting in truncations and indentations of the manipulated limbs (Kawakami et al., 2003), which mimics the effects of ridge removal or pharmacological inhibition of FGF or Ras/MAPK signalling. We observe identical phenotypes by silencing *flrt3* expression using RNAi technology. Not only AER markers are affected by *flrt3* silencing. The impairment of FGF signalling from the AER to the mesenchyme underneath provides also another evidence that ERK phosphorylation

is essential for AER integrity and activity. The importance of *flrt3* signalling from the ridge to the correct progress of the limb outgrowth becomes clear by observing how a small cluster of isolated AER cells is still able to promote outgrowth of part of the limb (Fig. 4F). The wide range of phenotypes observed is most probably due to the efficiency variability of both siRNA interference and electroporation. Notwithstanding, they all converge into the disruption of the AER integrity and consequent impairment of limb outgrowth.

Different studies have shown that *en-1* plays a role during migration and compaction of AER cells restricting the expression of *r-fng* and *wnt-7a* to the dorsal ectoderm (Loomis et al., 1998), while Wnt/ß-catenin signalling is required to maintain the AER after AER initiation and maturation (Barrow et al., 2003; Kengaku et al., 1998). Wnt-7a instructs the dorsal mesoderm to adopt dorsal characteristics, such as *lmx-1* expression, which in turn specifies dorsal pattern. Thus, *en-1* has a dual function in AER positioning and dorsal specification and hence acts to coordinate the two processes (Johnson and Tabin, 1997).

Overexpression of *flrt3* in the limb ectoderm produces *fgf8*-positive enlargements and projections of the pre-existing AER. The enlarged regions of the AER show also a broadening of the *fgf8* expression domain and a local inhibition of *en-1* expression (Fig. 2). *Flrt3*-electroporated limbs present a clear deregulation of the *en-1* ventral ectoderm territory. There is evidence that in mice lacking *en-1*, the correct positioning of the AER depends on correct *en-1* expression (Loomis et al., 1998, 1996) and that homozygous mice for a null allele of *en-1* present both DV and PD axes defects. The same phenotype is observed upon removal of *bmp2* and *bmp4* from the AER (Maatouk et al., 2009). In these mice, such as in *flrt3*-overexpressed chicken limbs, the AER is significantly broadened and *fgf8* expression is expanded, suggesting that the *en-1* domain may be affected by loss of BMP signalling from the AER.

Ectopic AERs induced upon *flrt3* overexpression are *fgf8*-positive in different extensions, being the most common phenotype the detection of *fgf8* mRNA only in the vicinity of the original AER (Figs. 2B arrows, 3A, B). The proximity to the pre-existent AER seems to be a key factor, suggesting that the cells that compose the ectopic structure are not completely committed to AER fate, denoting the presence of AER-like structures and emphasizing the importance of distinguishing between AER structure and function.

Therefore, *flrt3* seems to be necessary but not sufficient for proper AER formation and maintenance. This is supported by our observation that overexpression of *flrt3* in the flank between the forelimb and the hindlimb does not induce ectopic AERs, although the region has ectodermic competence for AER induction, as shown with FGF bead implantation in the flank (Cohn et al., 1995; Crossley et al., 1996; Mahmood et al., 1995; Mima et al., 1995; Vogel et al., 1996; Yonei-Tamura et al., 1999).

Our results also show that the projections from the pre-existing AER are not altered in their positional identity. *Lmx-1*, an established dorsal mesoderm identity marker, is absent from both sides of ventrally derived outgrowths. The same happens with *en-1* absence on dorsal outgrowths, suggesting a double-dorsal identity of those ectopic AERs.

BMP signalling, besides being essential for AER induction, is also necessary and sufficient to regulate *en-1* expression in the ventral ectoderm. Therefore, the loss of BMP signalling from the limb bud ectoderm results in failure of AER formation and bi-dorsal limbs (Ahn et al., 2001; Pizette et al., 2001; Soshnikova et al., 2003). This might explain the partial bi-dorsal identity in one of our *flrt3* electroporated limbs, probably through *gremlin*, a BMP signalling inhibitor known to promote a decrease in cell death and to expand the AER domain. In mice lacking AER BMP signalling, there is a failure in AER maturation and a subsequent loss of *en-1* and *msx2* in the AER. This promotes the expansion of the AER and the expression of FGF genes at high levels, decreasing *gremlin* in the distal mesenchyme and affecting the FGF/BMP loop (Maatouk et al., 2009).

The formation of perpendicular, connected or not, ridges after *flrt3* overexpression, is explained by Loomis' Zipper Hypothesis for the AER Maturation (Loomis et al., 1998). They propose a model that compares the final phase of AER constriction to the closing of a zipper, being the dorsal and ventral AER domains the two halves of the zipper. The zipping would occur with the dorsal half remaining relatively fixed and the ventral half being pulled towards it in a posterior-to-anterior fashion. Upon deregulation of *en-1*, the cells in the middle of the broadened AER are pulled towards the dorsal and ventral AER borders. In some cases distinct secondary AERs are formed due to the self-zipping of the ectopic rim. This theory supports the range of phenotypes observed upon *flrt3* overexpression.

Studies on *Xenopus* and mice show that *flrt3* expression can be induced by activation of FGF signalling (Bottcher et al., 2004; Haines et al., 2006). However, unpublished data from zebrafish *flrt3* by M. Fürthauer, B. Thisse, and C. Thisse (2005) suggest that in zebrafish FLRT3 may be involved in directing cell movements but do not appear to be related to the FGF pathway, since neither gain nor loss of FGF

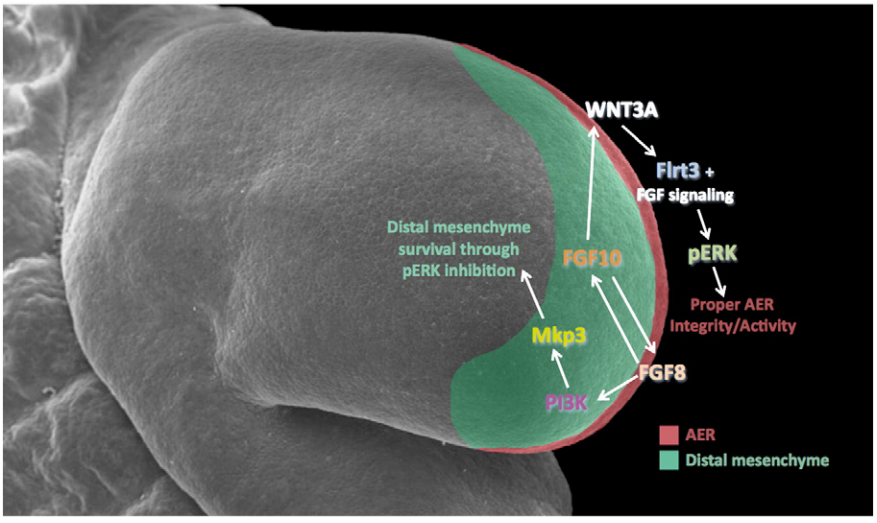

Fig. 6. Proposed model for *flrt3* role in chick limb bud development. FGF signaling from the AER maintains *fgf10* expression in the distal mesenchyme and induces PI3K signalling which is responsible for *Mkp3* activation. MKP3 would promote cell survival by inhibiting ERK activation. FGF activity from the distal mesenchyme induces *wnt3a* and *fgf8* at the AER. *Wnt3a* would be responsible for inducing *flrt3* expression and this, together with FGF signalling would activate ERK to maintain AER integrity and activity.

signalling appears to directly affect FLRT3 expression (Furthauer et al., 2002). In addition, *flrt3* expression is not increased in stem cells treated with FGFs and its antagonist (SU5402) (M. Mallo, personal communication). In our hands, no signs of *flrt3* induction by FGFs were obtained. Moreover, FGF8 appears to have a negative effect on *flrt3*. In fact, the FGF antagonist SU5402 does not reduce *flrt3* transcripts' level, as expected. Instead, it has no effect over *flrt3* expression. An interesting fact is that the *fgf8*-negative cells at the ectopic ridges, resulting from *flrt3* overexpression on the ectoderm, are able to induce ERK1/2 phosphorylation in the absence of FGF signalling, in contrast with what was described in xenopus (Bottcher et al., 2004).

Taking into account unpublished data on zebrafish and stem cells and our own data, we suggest that FLRT3 acts upstream of phospho-ERK1/2 and hypothesize that the FGF signalling pathway exerts a negative effect on *flrt3* expression, although an inhibition of the pathway is not enough to activate *flrt3* expression.

We have obtained ectopic *flrt3* induction around the WNT3A bead in a short time window, suggesting a direct activation of *flrt3* by WNT3A. *Wnt3a* signals through ß-catenin, being expressed in AER precursors and in the established AER (Kawakami et al., 2001; Kengaku et al., 1998). In fact, injection of RCAS dominant-active β-catenin into chick limb buds induces the appearance of ectopic ridge-like spikes (Capdevila et al., 1998; Kawakami et al., 2004). Therefore, we propose a direct induction of *flrt3* by *wnt3a*, even before it activates *fgf8* expression.

As already referred, BMPs are expressed in the AER and since they ensure the correct balance between apoptosis and survival of the AER cells, they are responsible for the integrity of the structure. BMP soaked beads applied into the developing limb promoted the inhibition of *flrt3* expression, but *mkp3* expression in the mesenchyme is not affected, suggesting that *flrt3* expression in the AER could be maintained by the activity of the BMP antagonist *gremlin* (Capdevila et al., 1999; Merino et al., 1999; Zuniga et al., 1999). Our results suggest that upon *flrt3* overexpression, an increase of *gremlin* expression and the subsequent loss of AER's BMP signalling affects cell death equilibrium at the AER resulting in a broadened AER. When *gremlin* expression disappears, BMP activity induces the regression of the AER and downregulation of *flrt3*.

In summary, *flrt3* is a key player during chicken limb development. Gain- and loss-of-function studies show that *flrt3* is necessary but not sufficient for proper AER formation and maintenance.

We favor a model (Fig. 6) in which FGF10 from the mesenchyme signals to the AER through *Wnt3a*, inducing FGF8 activity. Wnt3a would induce *flrt3* expression, and the FGF signalling, together with *flrt3* in the ectoderm, would activate ERK, thereby maintaining AER integrity. Simultaneously, FGF8 signals to the underlying mesenchyme via PI3K, inducing the expression of *mkp3*, thus promoting the survival of the distal mesenchymal cells.

Supplementary materials related to this article can be found online at doi:10.1016/j.ydbio.2011.04.031.

Acknowledgments

We would like to thank Adriana Lázaro Dominguez and Diana Chapela for excellent technical assistance, Angel Raya and Ana Tavares for providing pCAGGS expression vectors, Moisés Mallo for communicating unpublished results and to the members of the Organogenesis laboratory at IGC for their critical input. We also acknowledge the excellent technical assistance of the Electron Microscopy Unit of the Department de Anatomía Humana, Biología Celular y Zoología, Universidad de Extremadura. This work was supported by grants from EU (FP6-Cells into Organs), Fundação para a Ciência e a Tecnologia (FCT), Portugal (grants POCI/SAU-MMO/63284/2004 and PTDC/BIA-BCM/100867/2008), Ministerio de Ciencia e Innovación, Spain (Subprograma Ramon y Cajal, reference RYC-2008-02753) and by Centro de Biologia do Desenvolvimento, FCT, Portugal (POCTI-ISFL-4-664). A.R.T. was supported by fellowships from FCT (SFRH/BD/32346/2006) and Fundação Calouste Gulbenkian, Portugal. A.C.C. acknowledges fellowship SFRH/BPD/29957/2006 from FCT, Portugal. J.R.L. is supported by the Subprogram Ramón y Cajal from Ministerio de Ciencia e Innovación, Spain (RYC-2008-02753).

References

Ahn, K., Mishina, Y., Hanks, M.C., Behringer, R.R., Crenshaw III, E.B., 2001. BMPR-IA signaling is required for the formation of the apical ectodermal ridge and dorsal–ventral patterning of the limb. Development 128, 4449–4461.
Barrow, J.R., Thomas, K.R., Boussadia-Zahui, O., Moore, R., Kemler, R., Capecchi, M.R., McMahon, A.P., 2003. Ectodermal Wnt3/beta-catenin signaling is required for the establishment and maintenance of the apical ectodermal ridge. Genes Dev. 17, 394–409.
Boardman, P.E., Sanz-Ezquerro, J., Overton, I.M., Burt, D.W., Bosch, E., Fong, W.T., Tickle, C., Brown, W.R., Wilson, S.A., Hubbard, S.J., 2002. A comprehensive collection of chicken cDNAs. Curr. Biol. 12, 1965–1969.
Bottcher, R.T., Pollet, N., Delius, H., Niehrs, C., 2004. The transmembrane protein XFLRT3 forms a complex with FGF receptors and promotes FGF signalling. Nat. Cell Biol. 6, 38–44.
Boulet, A.M., Moon, A.M., Arenkiel, B.R., Capecchi, M.R., 2004. The roles of Fgf4 and Fgf8 in limb bud initiation and outgrowth. Dev. Biol. 273, 361–372.
Brummelkamp, T.R., Bernards, R., Agami, R., 2002. A system for stable expression of short interfering RNAs in mammalian cells. Science 296, 550–553.
Capdevila, J., Izpisua Belmonte, J.C., 2001. Patterning mechanisms controlling vertebrate limb development. Annu. Rev. Cell Dev. Biol. 17, 87–132.
Capdevila, J., Tabin, C., Johnson, R.L., 1998. Control of dorsoventral somite patterning by Wnt-1 and beta-catenin. Dev. Biol. 193, 182–194.
Capdevila, J., Tsukui, T., Rodriquez Esteban, C., Zappavigna, V., Izpisua Belmonte, J.C., 1999. Control of vertebrate limb outgrowth by the proximal factor Meis2 and distal antagonism of BMPs by Gremlin. Mol. Cell 4, 839–849.
Carl, M., Wittbrodt, J., 1999. Graded interference with FGF signalling reveals its dorsoventral asymmetry at the mid-hindbrain boundary. Development 126, 5659–5667.
Cohn, M.J., Izpisua-Belmonte, J.C., Abud, H., Heath, J.K., Tickle, C., 1995. Fibroblast growth factors induce additional limb development from the flank of chick embryos. Cell 80, 739–746.
Corson, L.B., Yamanaka, Y., Lai, K.M., Rossant, J., 2003. Spatial and temporal patterns of ERK signaling during mouse embryogenesis. Development 130, 4527–4537.
Crossley, P.H., Minowada, G., MacArthur, C.A., Martin, G.R., 1996. Roles for FGF8 in the induction, initiation, and maintenance of chick limb development. Cell 84, 127–136.
Dikic, I., Giordano, S., 2003. Negative receptor signalling. Curr. Opin. Cell Biol. 15, 128–135.
Eblaghie, M.C., Lunn, J.S., Dickinson, R.J., Munsterberg, A.E., Sanz-Ezquerro, J.J., Farrell, E.R., Mathers, J., Keyse, S.M., Storey, K., Tickle, C., 2003. Negative feedback regulation of FGF signaling levels by Pyst1/MKP3 in chick embryos. Curr. Biol. 13, 1009–1018.
Egea, J., Erlacher, C., Montanez, E., Burtscher, I., Yamagishi, S., Hess, M., Hampel, F., Sanchez, R., Rodriguez-Manzaneque, M.T., Bosl, M.R., Fassler, R., Lickert, H., Klein, R., 2008. Genetic ablation of FLRT3 reveals a novel morphogenetic function for the anterior visceral endoderm in suppressing mesoderm differentiation. Genes Dev. 22, 3349–3362.
Fernandez-Teran, M., Ros, M.A., 2008. The Apical Ectodermal Ridge: morphological aspects and signaling pathways. Int. J. Dev. Biol. 52, 857–871.
Furthauer, M., Lin, W., Ang, S.L., Thisse, B., Thisse, C., 2002. Sef is a feedback-induced antagonist of Ras/MAPK-mediated FGF signalling. Nat. Cell Biol. 4, 170–174.
Furushima, K., Yamamoto, A., Nagano, T., Shibata, M., Miyachi, H., Abe, T., Ohshima, N., Kiyonari, H., Aizawa, S., 2007. Mouse homologues of Shisa antagonistic to Wnt and Fgf signalings. Dev. Biol. 306, 480–492.
Ganan, Y., Macias, D., Duterque-Coquillaud, M., Ros, M.A., Hurle, J.M., 1996. Role of TGF beta s and BMPs as signals controlling the position of the digits and the areas of interdigital cell death in the developing chick limb autopod. Development 122, 2349–2357.
Geetha-Loganathan, P., Nimmagadda, S., Huang, R., Scaal, M., Christ, B., 2006. Expression pattern of BMPs during chick limb development. Anat. Embryol. (Berl) 211 (Suppl 1), 87–93.
Haines, B.P., Wheldon, L.M., Summerbell, D., Heath, J.K., Rigby, P.W., 2006. Regulated expression of FLRT genes implies a functional role in the regulation of FGF signalling during mouse development. Dev. Biol. 297, 14–25.
Hamburger, V., Hamilton, H.L., 1951. A series of normal stages in the development of the chick embryo. J. Morphol. 88, 49–92.
Johnson, R.L., Tabin, C.J., 1997. Molecular models for vertebrate limb development. Cell 90, 979–990.
Kawakami, Y., Capdevila, J., Buscher, D., Itoh, T., Rodriguez Esteban, C., Izpisua Belmonte, J.C., 2001. WNT signals control FGF-dependent limb initiation and AER induction in the chick embryo. Cell 104, 891–900.
Kawakami, Y., Rodriguez-Leon, J., Koth, C.M., Buscher, D., Itoh, T., Raya, A., Ng, J.K., Esteban, C.R., Takahashi, S., Henrique, D., Schwarz, M.F., Asahara, H., Izpisua Belmonte, J.C., 2003. MKP3 mediates the cellular response to FGF8 signalling in the vertebrate limb. Nat. Cell Biol. 5, 513–519.

Kawakami, Y., Esteban, C.R., Matsui, T., Rodriguez-Leon, J., Kato, S., Belmonte, J.C., 2004. Sp8 and Sp9, two closely related buttonhead-like transcription factors, regulate Fgf8 expression and limb outgrowth in vertebrate embryos. Development 131, 4763–4774.

Kengaku, M., Capdevila, J., Rodriguez-Esteban, C., De La Pena, J., Johnson, R.L., Belmonte, J.C., Tabin, C.J., 1998. Distinct WNT pathways regulating AER formation and dorsoventral polarity in the chick limb bud. Science 280, 1274–1277.

Khokha, M.K., Hsu, D., Brunet, L.J., Dionne, M.S., Harland, R.M., 2003. Gremlin is the BMP antagonist required for maintenance of Shh and Fgf signals during limb patterning. Nat. Genet. 34, 303–307.

Kurose, H., Bito, T., Adachi, T., Shimizu, M., Noji, S., Ohuchi, H., 2004. Expression of Fibroblast growth factor 19 (Fgf19) during chicken embryogenesis and eye development, compared with Fgf15 expression in the mouse. Gene Expr. Patterns 4, 687–693.

Lacy, S.E., Bonnemann, C.G., Buzney, E.A., Kunkel, L.M., 1999. Identification of FLRT1, FLRT2, and FLRT3: a novel family of transmembrane leucine-rich repeat proteins. Genomics 62, 417–426.

Lewandoski, M., Sun, X., Martin, G.R., 2000. Fgf8 signalling from the AER is essential for normal limb development. Nat. Genet. 26, 460–463.

Lizarraga, G., Ferrari, D., Kalinowski, M., Ohuchi, H., Noji, S., Kosher, R.A., Dealy, C.N., 1999. FGFR2 signaling in normal and limbless chick limb buds. Dev. Genet. 25, 331–338.

Logan, M., 2003. Finger or toe: the molecular basis of limb identity. Development 130, 6401–6410.

Loomis, C.A., Kimmel, R.A., Michaud, J., Wurst, W., Hanks, M., Joyner, A.L., 1996. The mouse Engrailed-1 gene and ventral limb patterning. Nature 382, 360–363.

Loomis, C.A., Kimmel, R.A., Tong, C.X., Michaud, J., Joyner, A.L., 1998. Analysis of the genetic pathway leading to formation of ectopic apical ectodermal ridges in mouse Engrailed-1 mutant limbs. Development 125, 1137–1148.

Lunn, J.S., Fishwick, K.J., Halley, P.A., Storey, K.G., 2007. A spatial and temporal map of FGF/Erk1/2 activity and response repertoires in the early chick embryo. Dev. Biol. 302, 536–552.

Maatouk, D.M., Choi, K.S., Bouldin, C.M., Harfe, B.D., 2009. In the limb AER Bmp2 and Bmp4 are required for dorsal–ventral patterning and interdigital cell death but not limb outgrowth. Dev. Biol. 327, 516–523.

Mahmood, R., Bresnick, J., Hornbruch, A., Mahony, C., Morton, N., Colquhoun, K., Martin, P., Lumsden, A., Dickson, C., Mason, I., 1995. A role for FGF-8 in the initiation and maintenance of vertebrate limb bud outgrowth. Curr. Biol. 5, 797–806.

Maretto, S., Muller, P.S., Aricescu, A.R., Cho, K.W., Bikoff, E.K., Robertson, E.J., 2008. Ventral closure, headfold fusion and definitive endoderm migration defects in mouse embryos lacking the fibronectin leucine-rich transmembrane protein FLRT3. Dev. Biol. 318, 184–193.

Mariani, F.V., Ahn, C.P., Martin, G.R., 2008. Genetic evidence that FGFs have an instructive role in limb proximal–distal patterning. Nature 453, 401–405.

Martin, G.R., 1998. The roles of FGFs in the early development of vertebrate limbs. Genes Dev. 12, 1571–1586.

Merino, R., Rodriguez-Leon, J., Macias, D., Ganan, Y., Economides, A.N., Hurle, J.M., 1999. The BMP antagonist Gremlin regulates outgrowth, chondrogenesis and programmed cell death in the developing limb. Development 126, 5515–5522.

Mima, T., Ohuchi, H., Noji, S., Mikawa, T., 1995. FGF can induce outgrowth of somatic mesoderm both inside and outside of limb-forming regions. Dev. Biol. 167, 617–620.

Montero, J.A., Ganan, Y., Macias, D., Rodriguez-Leon, J., Sanz-Ezquerro, J.J., Merino, R., Chimal-Monroy, J., Nieto, M.A., Hurle, J.M., 2001. Role of FGFs in the control of programmed cell death during limb development. Development 128, 2075–2084.

Niswander, L., Martin, G.R., 1992. Fgf-4 expression during gastrulation, myogenesis, limb and tooth development. Development 114, 755–768.

Pizette, S., Abate-Shen, C., Niswander, L., 2001. BMP controls proximodistal outgrowth, via induction of the apical ectodermal ridge, and dorsoventral patterning in the vertebrate limb. Development 128, 4463–4474.

Pott, U., Fuss, B., 1995. Two-color double in situ hybridization using enzymatically hydrolyzed nonradioactive riboprobes. Anal. Biochem. 225, 149–152.

Raible, F., Brand, M., 2001. Tight transcriptional control of the ETS domain factors Erm and Pea3 by Fgf signaling during early zebrafish development. Mech. Dev. 107, 105–117.

Savage, M.P., Fallon, J.F., 1995. FGF-2 mRNA and its antisense message are expressed in a developmentally specific manner in the chick limb bud and mesonephros. Dev. Dyn. 202, 343–353.

Sivak, J.M., Petersen, L.F., Amaya, E., 2005. FGF signal interpretation is directed by Sprouty and Spred proteins during mesoderm formation. Dev. Cell 8, 689–701.

Smith, T.G., Tickle, C., 2006. The expression of Flrt3 during chick limb development. Int. J. Dev. Biol. 50, 701–704.

Smith, T.G., Karlsson, M., Lunn, J.S., Eblaghie, M.C., Keenan, I.D., Farrell, E.R., Tickle, C., Storey, K.G., Keyse, S.M., 2006. Negative feedback predominates over cross-regulation to control ERK MAPK activity in response to FGF signalling in embryos. FEBS Lett. 580, 4242–4245.

Soshnikova, N., Zechner, D., Huelsken, J., Mishina, Y., Behringer, R.R., Taketo, M.M., Crenshaw III, E.B., Birchmeier, W., 2003. Genetic interaction between Wnt/beta-catenin and BMP receptor signaling during formation of the AER and the dorsal–ventral axis in the limb. Genes Dev. 17, 1963–1968.

Sun, X., Mariani, F.V., Martin, G.R., 2002. Functions of FGF signalling from the apical ectodermal ridge in limb development. Nature 418, 501–508.

Thisse, B., Thisse, C., 2005. Functions and regulations of fibroblast growth factor signaling during embryonic development. Dev. Biol. 287, 390–402.

Tickle, C., 2002. Molecular basis of vertebrate limb patterning. Am. J. Med. Genet. 112, 250–255.

Trokovic, R., Trokovic, N., Hernesniemi, S., Pirvola, U., Vogt Weisenhorn, D.M., Rossant, J., McMahon, A.P., Wurst, W., Partanen, J., 2003. FGFR1 is independently required in both developing mid- and hindbrain for sustained response to isthmic signals. EMBO J. 22, 1811–1823.

Tsang, M., Dawid, I.B., 2004. Promotion and attenuation of FGF signaling through the Ras-MAPK pathway. Sci. STKE pe17.

Vogel, A., Rodriguez, C., Izpisua-Belmonte, J.C., 1996. Involvement of FGF-8 in initiation, outgrowth and patterning of the vertebrate limb. Development 122, 1737–1750.

Wilkinson, D.G., 1992. In Situ Hybridization. Oxford Univ. Press, Oxford.

Xu, X., Weinstein, M., Li, C., Naski, M., Cohen, R.I., Ornitz, D.M., Leder, P., Deng, C., 1998. Fibroblast growth factor receptor 2 (FGFR2)-mediated reciprocal regulation loop between FGF8 and FGF10 is essential for limb induction. Development 125, 753–765.

Yonei-Tamura, S., Endo, T., Yajima, H., Ohuchi, H., Ide, H., Tamura, K., 1999. FGF7 and FGF10 directly induce the apical ectodermal ridge in chick embryos. Dev. Biol. 211, 133–143.

Zhang, S., Lin, Y., Itaranta, P., Yagi, A., Vainio, S., 2001. Expression of Sprouty genes 1, 2 and 4 during mouse organogenesis. Mech. Dev. 109, 367–370.

Zuniga, A., Haramis, A.P., McMahon, A.P., Zeller, R., 1999. Signal relay by BMP antagonism controls the SHH/FGF4 feedback loop in vertebrate limb buds. Nature 401, 598–602.